

Single-Mode 850 nm VCSELs for 54 Gbit/sec On-Off Keying Transmission Over 1 km Multi-Mode Fiber

Kai-Lun Chi¹, Yi-Xuan Shi¹, Xin-Nan Chen¹, Jason (Jyehong) Chen², Ying-Jay Yang³, J.-R Kropp⁴, N. Ledentsov Jr.⁴, M. Agustin⁴, N.N. Ledentsov⁴, *Senior Member IEEE*, G. Stepniak⁵, J. P. Turkiewicz⁵ and Jin-Wei Shi^{1*}, *Senior Member IEEE*

Abstract— By combing Zn-diffusion and oxide-relief apertures with strong detuning (> 20 nm) in our demonstrated short-cavity ($\lambda/2$) 850nm vertical-cavity surface-emitting lasers (VCSELs), wide electrical-to-optical bandwidth (29-24 GHz), low differential resistance ($\sim 100 \Omega$), and (quasi) single-mode (SM) with reasonable output power (~ 1.4 mW) performances can be simultaneously achieved. Error-free on-off keying transmission at 54 Gbit/sec data rate through 1 km OM4 multi-mode fiber (MMF) can be achieved by using highly SM device with forward error correction and decision feedback equalization techniques. As compared to the reference device with a larger oxide-relief aperture and multi-mode performance, the SM device exhibits lower bit-error-rate (1×10^{-5} vs. 1×10^{-2}) at 54 Gbit/sec. This result indicates that modal dispersion plays more important role in transmission than that of output power does. We benchmark these results to an industrial 50 Gbit/sec SM VCSEL. It shows a higher bit-error-rate value $\sim 3.5 \times 10^{-3}$ vs. $\sim 1.4 \times 10^{-4}$ under the same received optical power.

Keywords: Semiconductor lasers, Vertical cavity surface emitting lasers

I. INTRODUCTION

Vertical-cavity surface-emitting lasers (VCSELs) with central wavelength at 850 nm has become the most important light source in the booming market of short-reach (< 300 meters) optical interconnect (OI) [1]. The next generation interconnect framework has been targeted at data rate per channel as high as 56 Gbit/sec (CEI (Common Electrical Interface)-56G) [2] with the total data rate up to 400 Gbit/sec. To further boost the modulation speed and reduce the energy consumption of the high-reliable VCSELs has thus become a major challenge for such application. Recently, by using highly strained active layer with short-cavity ($\lambda/2$) design, 850 nm VCSEL with state-of-the-art 3-dB modulation bandwidth up to 30 GHz for 50 Gbit/sec data transmission over 4 meter OM4 multi-mode fiber (MMF) has been demonstrated [3]. By combing the advanced feed-forward equalization (FFE) techniques with this kind of high-speed VCSEL in the transmitter side, data rate for error-free transmission can be further boosted to 71 Gbit/sec [4] (over 7 meter OM3 MMF). Nevertheless, modal dispersion in MMF would become an issue, which seriously limits the maximum linking distance under such high transmission data rate.

¹Kai-Lun Chi, Yi-Xuan Shi, Xin-Nan Chen, and Jin-Wei Shi are with the Department of Electrical Engineering, National Central University, Taoyuan 320, Taiwan. (e-mail: jwshi@ee.ncu.edu.tw). ²Jason (Jyehong) Chen is with the Department of Photonics, National Chiao-Tung University, Hsinchu 300, Taiwan. ³Ying-Jay Yang is with the Department of Electrical Engineering, National Taiwan University, Taipei, 106, Taiwan. ⁴J.-R Kropp, N. Ledentsov Jr., M. Agustin and N.N. Ledentsov are with the VI Systems GmbH, Hardenbergstr. 7, Berlin 10623, Germany. ⁵G. Stepniak and J. P. Turkiewicz are with the Institute of Telecommunications, Warsaw University of Technology, ul. Nowowiejska 15/19, 00-661 Warsaw, Poland.

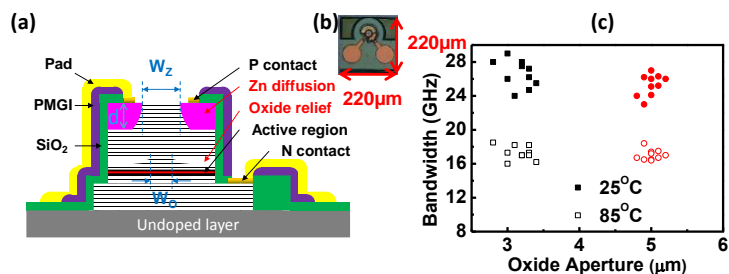


Figure 1. (a) Conceptual cross-sectional views of demonstrated VCSELs. (b) Top-view of fabricated VCSEL chip. PMGI: polymethylglutarimide. (c) Measured 3-dB E-O bandwidths of VCSELs with two different oxide-relief apertures (black: $\sim 3 \mu\text{m}$; red: $\sim 5 \mu\text{m}$ aperture sizes) under RT (solid symbols) and 85°C (open symbols) operations.

The reported linking distance through OM4 MMF for >50 Gbit/sec data transmission by use of multi-mode (MM) VCSEL and FFE technique is usually less than 60 meter [2-5]. Such number usually can't satisfy the requirement of modern datacenters, where over 50 meter to 1-2 km linking distance is necessary due to the tremendously increase in the size of data center [6].

Using high-speed and (quasi) single-mode (SM) VCSEL [7-10] and FFE [2-5,11] (also decision feedback equalization (DFE) techniques [11]) are all promising solutions to further extend the transmission distance through MMF. However, SM performance in VCSEL usually induces a low-frequency roll-off in its electrical-to-optical (E-O) frequency response, which limits its maximum 3-dB bandwidth and significantly degrade the quality of eye-patterns [7]. In addition, the FFE/DFE techniques would definitely increase the cost and power consumption of OI system. Fortunately, these two factors may go down by 40% with each new IC generation [12]. Having linking distance up to km at very-high data rate (~ 50 Gbit/sec) based on 850 nm VCSEL allows to use the installed MMF infrastructure in data center without wavelength conversion to 1.3-1.55 μm for long-reach single-mode fiber (SMF) transmission. Such wavelength conversion would result in the additional electronic/optoelectronic costs and energy consumptions. Furthermore, making seamless 850nm MMF network additionally reduces latency as no wavelength conversion stage is needed.

In this letter, we demonstrated a novel (quasi-)SM 850 nm VCSEL structure to further enhance the transmission performance of 54 Gbit/sec data. By combing $\lambda/2$ short-cavity, Zn-diffusion and oxide-relief apertures with strong detuning (> 20 nm) between Fabry-Perot (FP) cavity mode and gain peak wavelengths of multiple quantum wells (MQWs) [13], our demonstrated 850 nm VCSELs cannot only achieve (quasi-)SM performance but also sustain very-high speed performance (~ 28

GHz 3-dB E-O bandwidth) with a reasonable output power (1.4 mW at 6 mA bias). By use of these (quasi-)SM high-speed VCSELs, 54 Gbit/sec error-free transmission through 1 km OM4 MMF with use of DFE and forward error correction (FEC) (with a 7% overhead) techniques have been successfully achieved. We benchmark these results to the data obtained for industrial quasi-SM VCSELs from VI-Systems GmbH¹ (V50-850M), which is designed for 50 Gbit/sec data transmission [10], and our demonstrated SM device shows a lower bit-error-rate (BER) (1.3×10^{-4} vs. 3.5×10^{-3}) under the same setup and received optical power (-8 dBm).

II. DEVICE STRUCTURE

Figures 1 (a) and (b) show conceptual cross-sectional and top views of the studied device, respectively. With additional Zn-diffusion apertures in the top p-type DBR layers, we can not only manipulate the number of optical transverse modes inside VCSEL cavity but also reduce the differential resistance [7,9,13]. In addition, the oxide layer for current confinement is removed from our oxide-relief structure by using selective wet chemical etching [7,9,13] to reduce its parasitic capacitance [9]. The diameters of the Zn-diffusion (W_z) and oxide-relief apertures (W_o) of the measured devices are specified in the figures below. In this work, devices with SM performance have values of W_z , W_o , and Zn-diffusion depths (d) of 7, 3, and 1 μm , respectively. On the other hand, the MM reference devices have the same W_z and d but with a larger oxide-relief diameter W_o as 5 μm . The fabricated device has a $\sim 23 \mu\text{m}$ diameter active mesa, which is integrated with the slot line pads for on-wafer high-speed measurement, as shown in Figure 1(b). The detail fabrication process can be referred to our previous work [9,13]. The epi-layer structure, purchased from LandMark², is grown on a semi-insulating GaAs substrate, which is composed of three $\text{In}_{0.1}\text{Ga}_{0.9}\text{As}/\text{Al}_{0.3}\text{Ga}_{0.7}\text{As}$ (40/80 \AA) MQWs sandwiched between a 36-pair n-type and 26-pair p-type $\text{Al}_{0.9}\text{Ga}_{0.1}\text{As}/\text{Al}_{0.12}\text{Ga}_{0.88}\text{As}$ Distributed-Bragg-Reflector (DBR) layers with an $\text{Al}_{0.98}\text{Ga}_{0.02}\text{As}$ layer (50 nm thickness) above the MQWs for oxidation. Compared with previous work [7,9], the thickness of the cavity layer has been further downscaled from 1.5 to 0.5 λ , which shortens the internal carrier transit time [13]. Here, λ is the operating wavelength inside the VCSEL cavity. Due to the increase in the transit-time limited bandwidth, the low-frequency roll-off [7], which is usually the major bandwidth limiting factor of a single-mode VCSEL, can be minimized [13]. The Fabry-Perot (FP) dip mapping of the whole VCSEL wafer shows that the cavity resonant wavelength locates at around 860 nm and the detuning between the gain peak (839 nm) and FP dip (~ 860 nm) wavelengths is as large as around 20 nm. Such strong detuning would result in significant improvement in 3-dB O-E bandwidth of VCSEL due to the device self-heating induced red-shift of gain peak under high bias current [13]. Figure 1 (c) shows the collections of measured 3-dB E-O bandwidths of several (quasi-) SM ($W_o=3 \mu\text{m}$) and MM ($W_o=5 \mu\text{m}$) devices measured at room-temperature (RT) and 85 $^\circ\text{C}$ operations, which will be discussed in detail latter.

III. MEASUREMENT RESULTS

The light output and bias voltages versus current (L-I and V-I)

characteristics of VCSELs with quasi-SM ($W_o=3 \mu\text{m}$) and MM ($W_o=5 \mu\text{m}$) performances are shown in Figures 2 (a) and (b), respectively. Both devices share the same geometric size (W_z , and d) except for W_o . Although it is doable to achieve highly SM performance in our device structure by choosing the size of W_o larger than W_z , which can induce significant intra-cavity loss and strongly suppress the higher order-modes [7]. However, this approach would degrade the maximum 3-dB E-O bandwidth of SM VCSEL [7,14]. Furthermore, the strong optical feedback of highly SM device would usually result in the degradation of eye-patterns during data transmission [7]. Three typical measured traces (devices A to C and D to F) are shown in each figure. Thanks to our Zn-diffusion process, the measured differential resistance of devices A to C, even with such a small oxide-relief aperture, can be as low as 70~100 Ω . This is much smaller than the values typically reported ($>150 \Omega$) for high-speed VCSELs at 850 nm with a similar size of current-confined aperture [1].

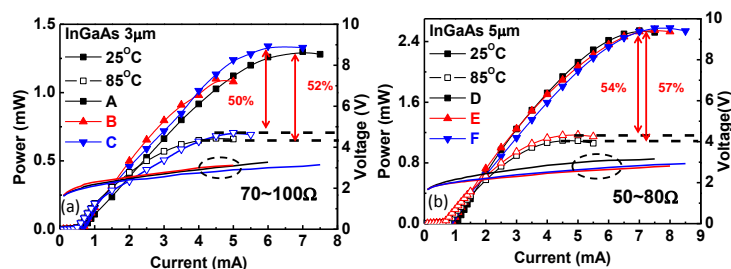


Figure 2. Measured L-I-V curves of VCSELs with oxide-relief apertures of (a) 3 μm (devices A to C), (b) 5 μm (devices D to F). The range of the measured differential resistance is specified on I-V curves. Solid and open symbols in L-I curves represent the measured power at RT and 85 $^\circ\text{C}$, respectively.

The L-I curves with solid and open symbols represent the measurement results at RT and 85 $^\circ\text{C}$ operation, respectively. We can clearly see that devices under 85 $^\circ\text{C}$ operation exhibit smaller threshold current than those of devices under RT operation. This can be attributed to the strong wavelength detuning in our VCSEL structure as discussed before. The inset in Figure 3 (a) shows the measured L-I-V curves of reference 50 Gbit/sec VCSEL with quasi-SM performance provided by VIS Company (V50-850 M) under room temperature operation. We can clearly see that both quasi-SM devices have a very close L-I curve, which includes the same maximum saturation bias current ($\sim 5\text{mA}$) and output power (~ 1.5 mW), but reference device has a smaller threshold current (0.2 vs. 0.5 mA). This might be attributed to the smaller detuning wavelengths between gain peak and FP dip (15 vs. 20 nm) in reference. In addition, thanks to the Zn-diffusion process, a significant reduction in the measured differential resistance (~ 200 vs. 70~100 Ω) of home-made devices with additional Zn-diffusion apertures can be observed.

The high-speed E-O performance of the fabricated devices was measured by a lightwave component analyzer (LCA), which was composed of a network analyzer (Anritsu 37397C) and a calibrated 25GHz photoreceiver module (New focus 1481-S). Figures 4 and 5 show the measured typical bias dependent E-O frequency responses and output optical spectra of devices A (quasi-SM) and D (MM), respectively under RT operation. We can clearly see that devices A and D shows a very close maximum 3-dB E-O bandwidth value at around 28

¹VI Systems GmbH, Hardenbergstr. 7, Berlin 10623, Germany. Name of Product: V50-850M

²LandMark Optoelectronics Corporation, No.12, Nanke 9th Rd., Shanhua Dist., Tainan City 741, Taiwan.

> REPLACE THIS LINE WITH YOUR PAPER IDENTIFICATION NUMBER (DOUBLE-CLICK HERE TO EDIT) < 3

and 27 GHz, respectively. Furthermore, device A exhibits quasi-SM behavior with around 8 dB side-mode suppression ratio (SMSR) under 6 mA bias current. Here, the SMSR value of each trace of quasi-SM device is specified. Such value in SM VCSEL has determinant effect on the transmission performance through MMF [7,8]. On the other hand, for the case of MM VCSEL (devices D), the root mean square (RMS) optical spectral width in each trace is specified. As opposite to that SMSR is applicable to SM VCSEL, when MM VCSEL has many modes of comparable intensity, which would all have significant contribution to transmission, the RMS spectral width value is a much more physical parameter than that of SMSR. As shown in Figure 1 (c), the measured E-O bandwidths under RT operations of quasi-SM and MM devices range from 29-24 and 27-23 GHz, respectively. In addition, when the ambient temperature reaches 85°C, both devices have 3-dB bandwidths at around 16~18 GHz. Such distribution in device's speed performance is mainly due to the process variation in oxide-apertures during mesa wet etching and oxidation. In addition, for the VCSEL structure we demonstrated here, there is a trade-off between SMSR and speed performance [14]. Our devices can have a perfect SM characteristic (SMSR > 30 dB) under the full range of bias current at the expense of a smaller 3-dB E-O bandwidth (~24 GHz), which will be discussed latter.

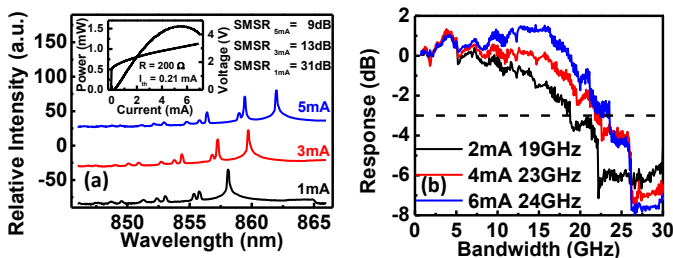


Figure 3. (a) Measured bias dependent output optical spectra and (b) measured E-O frequency responses under different bias currents of reference device (VIS: V50-850M). The inset to (a) shows the measured L-I-V curves of such device measured at RT.

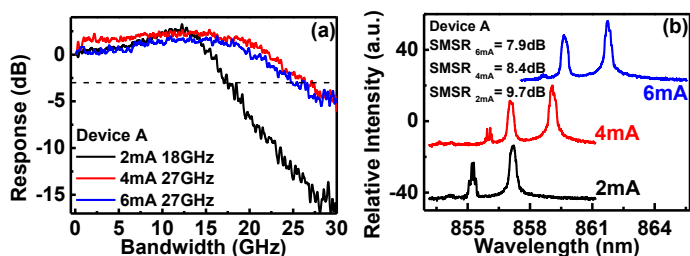


Figure 4. (a) E-O frequency responses of device A (quasi-SM) measured under different bias currents and RT operation. (b) The corresponding bias dependent output optical spectra.

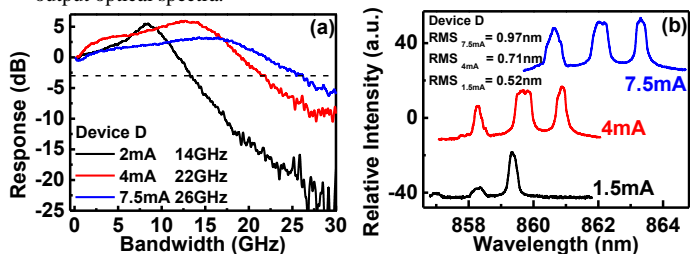


Figure 5. (a) E-O frequency responses of device D (MM) measured under different bias currents and RT operation. (b) The corresponding bias dependent output optical spectra.

Figure 3 (a) and (b) shows the measured typical bias dependent output optical spectra and E-O frequency responses of reference V50-850M, respectively. We can clearly see that compared with that of our home-made (MM and quasi-SM) VCSELs, its measured 3-dB E-O bandwidth is smaller (~24 vs. ~27 GHz) but it has a higher SMSR under maximum bias current (10 vs. 8 dB). According to these above-mentioned static measurement results, the extracted thermal resistances of such three kinds of VCSELs are almost the same as around 3.1 K/mW. Figure 6 (a) shows the measured received light output power vs. BER (after DFE process) of home-made SM (NCU_SM), MM (NCU_MM), and reference V50-850M (VIS_SM) devices measured at 54 Gbit/sec under back-to-back (BTB) and through 1 km OM4 fiber data transmission. Here, home-made device (NCU_SM) with a perfect SM performance but a slightly degraded 3-dB E-O bandwidth (~24 GHz) is chosen for this transmission experiment and it's measured bias dependent output optical spectra with L-I-V curve is given in Figure 6 (b). We can clearly see that under full range of bias current, highly SM characteristic (SMSR > 30 dB) can be sustained, which is superior to that of VIS reference device, as discussed in Figure 3 (a).

The 54 Gbit/sec data rate adapted 50 Gbit/sec payload and 7% forward error correction (FEC) overhead. 54 Gbit/s non-return-to-zero (NRZ) electrical signal with pseudo-random binary sequence (PRBS) length of $2^{15}-1$ is generated through SHF 12100B Bit Pattern Generator. All the devices are tested under the same peak-to-peak driving voltage (0.45 V) and the optimized bias current for lowest BER values of MM, SM, and V50-850 M is 6, 3, and 2 mA, respectively. The VCSELs under test are connected to an OM4 MMF with 1 km length. A photo-receiver module (New Focus; 1484-A-50) with a 22 GHz bandwidth and 80 V/W conversion gain is adopted in our receiving side. The output signal from receiver was captured in the Tektronix DPO 73304D real time oscilloscope for further offline signal processing. The offline processing involves signal resampling at twice the bit rate, synchronization and decision feedback equalization (DFE) with 40 T/2 forward taps and 10 feedback taps. The equalizer is trained with recursive least squares (RLS) algorithm using a training sequence consisting of 3900 first bits of the PRBS. Q-parameter is used for the calculation of BER. Such approach is well accepted in the BER calculation of 850 nm VCSEL based transmission through MMF [15].

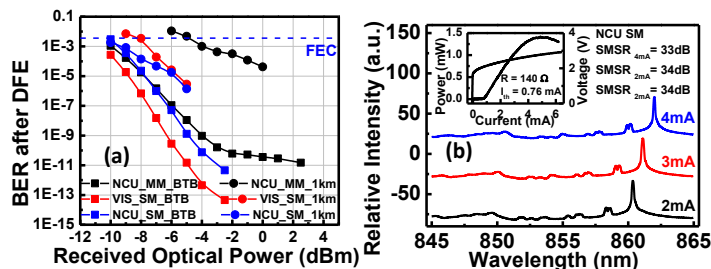


Figure 6. (a) Received optical power vs. BER for MM and (quasi-)SM VCSELs devices for BTB and over 1 km OM4 fiber transmission at 54 Gbit/sec. (b) The measured bias dependent output optical spectra of home-made highly-SM device chosen for transmission experiment. The inset shows its L-I-V curve.

As shown in Figure 6 (a), we can clearly see that even for the cases for BTB transmission, DFE processing is still necessary

to get (nearly) error-free ($BER < 1 \times 10^{-12}$) performance. This is because that the bandwidths of our VCSELs and receiver modules are marginal to have 54 Gbit/sec error-free transmission without using any signal processing techniques. For the case of 1 km transmission, BER values obtained for MM and two kinds of (quasi-)SM devices are all below FEC threshold ($BER = 3.8 \times 10^{-3}$), therefore error-free 1 km transmission can be achieved once FEC and DFE are used. However, compared with the case of BTB transmission, there is a more serious power penalty in MM devices for error-free performance. This result indicates that modal dispersion instead of output power of VCSELs plays a more important role in determining the maximum possible transmission distance for such high data rate (54 Gbit/sec) [9]. Additionally, we can clearly see that the performance in BER value (under the same received power as -8 dBm) after 1 km transmission is improved (1.4×10^{-4} vs. 3.5×10^{-3}) in the newly demonstrated oxide-relief/Zn-diffusion VCSELs as compared to that of reference SM (V50-850M). Such improvement can be attributed to its superior single-mode performance as discussed in Figure 6 (b). Figure 7 (a) and (b) shows the corresponding eye diagrams of SM, MM VCSELs, and reference device (V50-850M) for the case of BTB and 1 km OM4 fiber transmission, respectively.

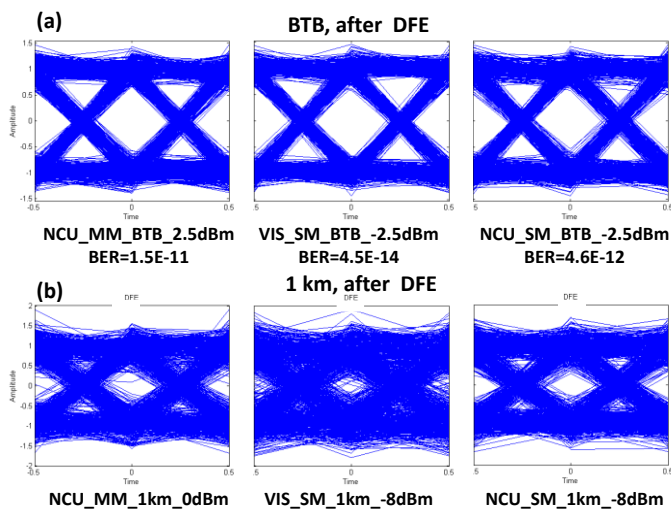


Figure 7. Measured 54 Gbit/s eye diagrams (after DFE processing) of (quasi-) SM and MM VCSELs for (a) BTB and (b) through 1km OM4 fiber.

IV. CONCLUSION

By performing Zn-diffusion, oxide-relief, and strong detuning techniques onto our demonstrated 850 nm VCSEL, high-speed (29-24 GHz) and (quasi-)SM performances with reasonable output power (1.4 mW at around 6 mA) can be achieved simultaneously. Compared with MM and quasi-SM references, which have close 3-dB O-E bandwidths but higher output power, our highly SM device exhibits a smallest BER value through 1 km MMF under 54 Gbit/sec OOK modulation. This indicates that modal dispersion instead of output power plays a more important role in determining the maximum possible transmission distance for such high data rate (54 Gbit/sec).

Acknowledgement: This work was sponsored by the Ministry of Science and Technology in Taiwan under grants MOST 102 - 2221 - E - 008 - 092 - MY3 and MOST 103-2622-E-009-004-CC1. The authors would also like to thank Dr. Wei

Lin and Dr. Shu-Wei Chiu of LandMark Taiwan Ltd for their support in the epitaxial layer growth.

REFERENCES

- [1] P. Moser, P. Wolf, G. Larisch, H. Li, J. A. Lott, and D. Bimberg, "Energy-efficient oxide-confined high-speed VCSELs for optical interconnects," *Proc. SPIE, Vertical-Cavity Surface Emitting Lasers XVIII*, vol. 9001, pp. 900103, Feb., 2014.
- [2] D. M. Kuchta, A. V. Rylyakov, C. L. Schow, J. E. Proesel, C. W. Baks, P. Westbergh, J.S. Gustavsson, and A. Larsson, "A 50 Gb/s NRZ Modulated 850 nm VCSEL Transmitter Operating Error Free to 90 °C," *IEEE/OSA Journal of Lightwave Technology*, vol. 33, no. 4, pp. 802-810, Feb., 2015.
- [3] E. Haglund, P. Westbergh, J.S. Gustavsson, E.P. Haglund, A. Larsson, M. Geen, and A. Joe, "30 GHz bandwidth 850 nm VCSEL with sub-100 fJ/bit energy dissipation at 25-50 Gbit/s," *Electron. Lett.*, vol. 51, no. 14, pp. 1096-1098, July, 2015.
- [4] D. M. Kuchta, A. V. Rylyakov, F. E. Doany, C. L. Schow, J. E. Proesel, C. W. Baks, P. Westbergh, J.S. Gustavsson, and A. Larsson, "A 71-Gb/s NRZ Modulated 850-nm VCSEL-Based Optical Link," *IEEE Photon. Technol. Lett.*, vol. 27, pp.577-580, March, 2015.
- [5] D. M. Kuchta, A. V. Rylyakov, C. L. Schow, J. E. Proesel, C. Baks, P. Westbergh, J. S. Gustavsson, and A. Larsson, "64Gb/s Transmission over 57m MMF using an NRZ Modulated 850nm VCSEL," *Proc. OFC 2014, San Francisco, CA, USA, March, 2014*, pp. Th3C. 2.
- [6] C. F. Lam, H. Liu, B. Koley, X. Zhao, V. Kamalov, and V. Gill, "Fiber optic communication technologies: What's needed for datacenter network operations," *IEEE Commun. Mag.*, vol. 48, no. 7, pp. 32-39, July 2010.
- [7] Jin-Wei Shi, Zhi-Rui Wei, Kai-Lun Chi, Jia-Wei Jiang, Jih-Min Wun, I-Cheng Lu, Jason (Jyehong) Chen, and Ying-Jay Yang, "Single-Mode, High-Speed, and High-Power Vertical-Cavity Surface-Emitting Lasers at 850 nm for Short to Medium Reach (2 km) Optical Interconnects," *IEEE/OSA Journal of Lightwave Technology*, vol. 31, pp. 4037-4044, Dec., 2013.
- [8] R. Safaisini, E. Haglund, P. Westbergh, J.S. Gustavsson, and A. Larsson, "20 Gbit/s data transmission over 2 km multimode fibre using 850 nm mode filter VCSEL," *Electron. Lett.*, vol. 50, no. 1, pp. 40-42, Jan., 2014.
- [9] Jin-Wei Shi, Jih-Cheng Yan, Jih-Min Wun, Jason (Jyehong) Chen, Ying-Jay Yang, "Oxide-Relief and Zn-Diffusion 850 nm Vertical-Cavity Surface-Emitting Lasers with Extremely Low Energy-to-Data-Rate Ratios for 40 Gbit/sec Operations" *IEEE J. of Sel. Topics in Quantum Electronics*, vol. 19, pp. 7900208, March/April, 2013.
- [10] J.-R. Kropp, V. A. Shchukin, N. N. Ledentsov, Jr., G. Schaefer, N. N. Ledentsov, B. Wu, Q. Shaofeng, M. Yanan, F. Zhiyong, and J. P. Turkiewicz, "850 nm single mode VCSEL-based 25Gx16 transmitter/receiver boards for parallel signal transmission over 1 km of multimode fiber," *Proc. SPIE, Next-Generation Optical Networks for Data Centers and Short-Reach Links II*, vol. 9390, pp. 93900C, March, 2015.
- [11] I-Cheng Lu, Jin-Wei Shi, Hsing-Yu Chen, Chia-Chien Wei, Sheng-Fan Tsai, Dar-Zu Hsu, Zhi-Rui Wei, Jih-Min Wun, and Jyehong Chen, "Ultra Low Power VCSEL for 35-Gbps 500-m OM4 MMF Transmission Employing FFE/DFE Equalization for Optical Interconnects," *Proc. OFC 2013, Anaheim, CA, USA, March, 2013*, pp. JTh2A.75.
- [12] P. A. Milder, R. Bouziane, R. Koutsoyannis, C. R. Berger, Y. Benlachar, R. I. Killely, M. Glick, and J. C. Hoe, "Design and simulation of 25 Gb/s optical OFDM transceiver ASICs," *Opt. Exp.*, vol. 19, pp. B337-B342, Dec. 2011.
- [13] Kai-Lun Chi, Jia-Liang Yen, Jih-Min Wun, Jia-Wei Jiang, I-Cheng Lu, Jason (Jyehong) Chen, Ying-Jay Yang, and Jin-Wei Shi, "Strong Wavelength Detuning of 850 nm Vertical-Cavity Surface-Emitting Lasers for High-Speed (>40 Gbit/sec) and Low-Energy Consumption Operation," *IEEE J. of Sel. Topics in Quantum Electronics*, vol. 21, no. 6, pp. 1701510, Nov./Dec., 2015.
- [14] J.-W. Shi, C.-C. Chen, Y.-S. Wu, S.-H. Guol, and Ying-Jay Yang, "The Influence of Zn-Diffusion Depth on the Static and Dynamic Behaviors of Zn-Diffusion High-Speed Vertical-Cavity Surface-Emitting Lasers at a 850nm Wavelength," *IEEE J. Quantum, Electron.*, vol. 45, pp. 800-806, July, 2009.
- [15] K. Szczerba, P. Westbergh, J. Karout, J. S. Gustavsson, Å. Haglund, M. Karlsson, P. A. Andrekson, E. Agrell, and A. Larsson, "4-PAM for High-Speed Short-Range Optical Communications," *J. Opt. Comm. Netw.*, vol. 4, pp. 885-894, Nov., 2012.